Supporting Information

Kinkelin et al. 10.1073/pnas.1311010110

SI Materials and Methods

Protein Preparation. *Saccharomyces cerevisiae* 12-subunit RNA polymerase (Pol) II was prepared as described previously (1). Full-length Bye1 was cloned into pOPINF with an N-terminal hexahistidine tag and expressed in *Escherichia coli* BL21 (DE3) (Novagen). The culture was grown in lysogeny broth (LB) medium at 37 °C until an OD_{600} of 0.9 was reached, induced with 0.25 mM isopropyl β-D-1-thiogalactopyranoside (IPTG), and grown for 18 h at 20 °C. Cells were collected by centrifugation and flash-frozen. Protein was purified by nickel affinity, anion exchange, and size-exclusion chromatography. Cells were lysed by sonication in buffer A [20 mM Tris, pH 7.5, 100 mM NaCl, 10 μM $ZnCl_2$, 10% (vol/vol) glycerol, and 5 mM DTT, supplemented with 20 mM imidazole, 1 U/μL DNase (Fermentas) and 1× protease inhibitors (100× stock: 1.42 mg leupeptin, 6.85 mg pepstatin A, 850 mg PMSF, and 1,650 mg benzamidine in 50 mL ethanol)]. After centrifugation at 16,000 × *g* for 20 min, the cleared lysate was applied to a preequilibrated (buffer A) Ni-nitrilotriacetic acid (NTA) agarose column (Qiagen). The column was washed with 10 column volumes of buffer A containing 20 mM imidazole before stepwise elution of the protein with buffer A containing 50/100/200 mM imidazole. Fractions containing Bye1 were pooled and applied to a MonoQ 10/100 GL column (GE Healthcare) equilibrated in buffer A. The protein was eluted with a linear gradient from 100 mM to 1 M NaCl [buffer B, 20 mM Tris, pH 7.5, 1 M NaCl, 10 μM $ZnCl_2$, 10% (vol/vol) glycerol, and 5 mM DTT]. To remove any minor contaminants, a final size exclusion step using a Superdex 200 10/300 GL column (GE Healthcare) in 20 mM Tris, pH 7.5, 100 mM NaCl, 10 μM $ZnCl_2$, 10% (vol/vol) glycerol, and 5 mM DTT was carried out. Selenomethionine-substituted Bye1 was grown in 2 L SelenoMet Base, 100 mL nutrient mix (Molecular Dimensions), and 80 mg selenomethionine (Acros Organics) at 37 °C until absorbance at 600 nm of 0.6. IPTG (0.5 mM), 50 mg selenomethionine, 100 mg lysine, threonine, and phenylalanine (Sigma-Aldrich), and 50 mg leucin, isoleucin, and valin (Sigma-Aldrich) was added per 2L culture, and the culture was grown for a further 18 h at 20 °C. Protein was purified as above. Bye1 TFIIS-like domain (TLD) (residues 225–370) was expressed as a larger variant (residues 69–370) containing a protease cleavage site at the N-terminal border of the TLD and cloned into pOPINI with an N-terminal hexahistidine tag. The protein was expressed and purified as above except that buffers did not contain glycerol, and the protein was eluted from the Ni-NTA column with 200 mM imidazole. After ion exchange purification, 300 μg precission protease was added, and cleavage was carried out overnight at 4 °C. To separate the cleavage products, the protein was applied to a preequilibrated (buffer A) Ni-NTA column. Bye1 TLD could be collected in the flow-through fraction and was then applied to size-exclusion chromatography using a Superdex 75 10/300 GL column.

Surface Plasmon Resonance. Approximately 2,500 resonance units of yeast Pol II were immobilized in immobilization buffer (Na-acetate, pH 5) on the surface of a biosensor CM5 chip (Biacore) using the amine coupling kit (Biacore) (2, 3). Full-length recombinant Bye1 was injected for 60 s at 10 μL/min in running buffer [5 mM Hepes (pH 7.25 at 20 °C), 40 mM $(NH_4)_2SO_4$, 10 μM $ZnCl_2$, 5 mM DTT, and 0.005% P20] at different concentrations (19 nM to 20 μM). The complex was allowed to dissociate for 5 min between injections. Affinity was measured for three independent dilution series. Raw data were corrected for the bulk signal from buffer and by identical injection through a flow cell in which no Pol II was immobilized. Data were analyzed with BIAevaluation software (Biacore).

Crystallization and X-Ray Structure Determination. Complexes of Pol II and Bye1 were formed by incubating Pol II with a 10-fold molar amount of Bye1 at 4 °C overnight. For the elongation complex (EC) and the arrested complex (AC), purified Pol II (3.5 mg/mL) was mixed with a twofold molar excess of template (EC template, see ref. 4; AC template, see ref. 5) prepared as described previously (6), 8 mM magnesium chloride, and 2 mM cytidine 5′-triphosphate (CTD) (AC), and incubated for 1 h (EC) or 2 h (AC) at 20 °C before crystallization by vapor diffusion with 5–7% (wt/vol) PEG 6000, 200 mM ammonium acetate, 300 mM sodium acetate, 50 mM Hepes, pH 7.0, and 5 mM tris(2-carboxyethyl) phosphine hydrochloride (TCEP) as reservoir solution. Crystals were grown for 5–10 d and cryo-protected in mother solution supplemented with 22% (vol/vol) glycerol and containing 4 μM tailed template, 2 mM CTP, and 8 mM magnesium chloride (AC), followed by overnight incubation at 8 °C before harvesting and freezing in liquid nitrogen. Bye1 TLD or SeMet-substituted Bye1 TLD was added to the cryo-protectant at 1 mg/mL, and crystals were incubated overnight at 8 °C. For complexes containing α,β-Methyleneadenosine 5′-triphosphate (AMPCPP), Pol II was cocrystallized with nucleic acids in the presence of 8 mM magnesium chloride and was soaked with 2 mM AMPCPP in all cryo-protectant solutions. For cocrystallization of full-length Pol II and Bye1, purified Pol II (3.5 mg/mL) was mixed with a 10-fold molar excess of recombinant Bye1 and incubated overnight at 4 °C before crystallization by vapor diffusion with 750 mM tri-Na-citrate and 100 mM Hepes, pH 7.5, as the reservoir solution. Crystals were grown for 13 d and cryo-protected in 22% (vol/vol) glycerol, followed by 1-h incubation before harvesting and flash-freezing in liquid nitrogen. Diffraction data were collected at 100 K at beamline X06SA of the Swiss Light Source. Data were collected at 0.91887 Å, the K-absorption peak of bromine, and 0.9797 Å, the K-absorption peak of selenium. Structures were solved with molecular replacement using BUSTER (7) and the structure of 12-subunit Pol II (1WCM) as a search model. Refinement was performed using iterative cycles of model building in COOT (8) and restrained refinement in BUSTER.

Chromatin Fractionation. Strains used in yeast chromatin fractionation were derived from W303. Plasmids containing hemagglutinin (HA)-tagged, full-length Bye1, Bye1 ΔPHD (Δ1–177), and Bye1 ΔTLD (Δ177–354) (obtained from S. D. Hanes, Division of Infectious Disease, Wadsworth Center, New York State Department of Health, Albany, New York) (9) were transformed into WT yeast. Chromatin fractionation was performed using a combination of previously described methods (10, 11). Cells were grown in yeast extract peptone dextrose (YPD) from a starting OD_{600} of 0.25 to mid-log phase (OD_{600} ~ 1.0). Forty OD_{600} units of cells were harvested by centrifugation and resuspended in 10 mL of sterile water. Following another round of centrifugation, cells were resuspended in 10 mL spheroplasting buffer (SB) (1 M sorbitol, 20 mM Tris, pH 7.4), collected by centrifugation, and stored at −80 °C overnight. The cell pellets were then thawed on ice, resuspended in 1.5 mL pre-SB (20 mM Tris, pH 7.4, 2 mM EDTA, 100 mM NaCl, and 10 mM 2-mercaptoethanol), and transferred to a 2-mL microcentrifuge tube. Cells were allowed to mix for 10 min at room temperature on a rotating shaker. Cells were pelleted by a flash spin

in a microcentrifuge, and the buffer was aspirated. Cell pellets were washed briefly in 1.5 mL SB buffer and quickly centrifuged as before. The pellet was resuspended in 1 mL SB buffer, and 125 μL of 10 mg/mL Zymolyase 20T (Seikagaku Biobusiness) in SB buffer was added. The mixture was incubated at room temperature for 30–60 min on a rotating shaker. The spheroplasting progress was assessed by addition of 10 μL of cells to 1 mL 1% SDS and vortexing, followed by measuring the OD_{600} of the liquid. Once the OD_{600} measurement decreased by more than 80% of the starting value, spheroplasting was stopped with ice-cold SB buffer. Spheroplasts were pelleted at 300 × *g* for 5 min at 4 °C in a chilled microcentrifuge. The buffer was removed, and the pellet was gently resuspended in 1 mL lysis buffer (LB) (0.4 M sorbitol, 150 mM potassium acetate, 2 mM magnesium acetate, 20 mM Pipes-KOH, pH 6.8, 1 μg/mL leupeptin, 1 μg/mL pepstatin, 1 μg/mL aprotinin, and 1 mM PMSF) and pelleted as above. The LB buffer wash step was repeated. To lyse the cells, the pellet was gently resupended in 250 μL LB with 1% Triton X-100, transferred to a 1.5-mL microcentrifuge tube, and incubated on ice for 10 min with occasional gentle mixing. Following lysis, 125 μL was removed for the whole cell extract (WCE), and the remainder was centrifuged at 5,000 × *g* for 15 min at 4 °C. The supernatant was collected as the soluble fraction. The chromatin pellet was washed once by resuspension in 125 μL of LB buffer with 1% Triton X-100 and spun as in the previous step. The supernatant was discarded, and the chromatin pellet was resuspended in 125 μL of LB buffer with 1% Triton X-100. All samples were normalized to total protein content of WCE as determined using Bradford reagent (Bio-Rad). Normalized WCE and volume equivalents of the soluble and chromatin fractions were boiled in 1× SDS loading buffer, separated by 15% SDS/PAGE, and analyzed by immunoblotting with antibodies HA (MMS-101R; Covance), 1:1,000; histone 4 (H4; 05-858; Millipore), 1:1,000; and glucose-6-phosphate-1-dehydrogenase (G6DH; A9521; Sigma), 1:100,000.

Histone Peptide Microarrays. Full-length Bye1 (residues 1–594) and Bye1 PHD (residues 47–134) were expressed as glutathione S-transferase (GST)-fusions from exponentially growing (OD_{600} ~0.6) BL21 RIL cells by overnight induction with 0.4 mM IPTG at 16 °C. Cells were lysed by sonication in cold 1× PBS, pH 7.6, containing 1 mM (PHD) or 5 mM (full-length) DTT, 1 mM PMSF, 1 mM $ZnSO_4$, and 10% (vol/vol) glycerol (full-length only). Proteins were captured on GST-Bind Resin (Novagen) and eluted in buffer containing 50 mM Tris·HCl, pH 8.0, and 10 mM glutathione. Proteins were dialyzed into buffer containing 20 mM Tris·HCl, pH 8.0, 150 mM NaCl, and 1 mM DTT before microarray hybridization. Peptide synthesis and validation, microarray fabrication, effector protein hybridization and detection, and data analysis were performed essentially as described previously (12). Briefly, biotinylated histone peptides (Table S2) were printed on streptavidin-coated glass slides at high density (each peptide printed 24 times per array). GST-fusion proteins were hybridized overnight on the array at a final concentration of 1.6 μM. Bound protein was labeled with α-GST (Sigma) and α-AlexaFluor 647 (Invitrogen) antibodies, and interactions were visualized with a Typhoon Trio+ scanner (GE). Densitometry measurements were acquired using ImageQant TL (GE).

Synthetic Lethality Screen. Strains used to validate candidates from the synthetic lethality screens were derived from BY4741. Synthetic genetic array analysis was performed as described previously (13, 14). Briefly, strain BY5563 *bye1*Δ was crossed to the complete KO library of nonessential genes (15). After sporulation and selection for the respective double KO, the latter was screened for viability. The screen was performed on a Beckman-Coulter Biomek FX.

In Vitro Transcription Assay. Nuclear extracts of *BY4741* and *bye1Δ* were prepared from 3 L of yeast culture as described previously (16, 17). Activator-dependent in vitro transcription assays were carried out using 150 ng of recombinant full-length Gcn4 (18) and addition of recombinant Bye1. The transcript was detected by primer extension using the 5′-Cy5–labeled oligonucleotide 5′-TTCACCAGTGAGACGGGCAAC-3′ (16). The resulting gel was scanned on a typhoon scanner FLA9400, and data were analyzed with ImageQuant Software (GE Healthcare).

RNA Extension Assay. RNA extension assays were carried out as described previously (19). All samples were incubated overnight at 4 °C before addition of nucleoside triphosphates (NTPs) to allow complex formation of Pol II and Bye1.

ChIP and Gene Averaged Profiles. ChIP and generation of gene averaged profiles was carried out as described previously (20–22).

1. Sydow JF, et al. (2009) Structural basis of transcription: Mismatch-specific fidelity mechanisms and paused RNA polymerase II with frayed RNA. *Mol Cell* 34(6):710–721.
2. Johnsson B, Löfås S, Lindquist G (1991) Immobilization of proteins to a carboxymethyldextran-modified gold surface for biospecific interaction analysis in surface plasmon resonance sensors. *Anal Biochem* 198(2):268–277.
3. Löfås S, Johnsson B (1990) A novel hydrogel matrix on gold surfaces in surface plasmon resonance sensors for fast and efficient covalent immobilization of ligands. *J Chem Soc* 21:1526–1528.
4. Cheung AC, Sainsbury S, Cramer P (2011) Structural basis of initial RNA polymerase II transcription. *EMBO J* 30(23):4755–4763.
5. Cheung AC, Cramer P (2011) Structural basis of RNA polymerase II backtracking, arrest and reactivation. *Nature* 471(7337):249–253.
6. Kettenberger H, Armache KJ, Cramer P (2004) Complete RNA polymerase II elongation complex structure and its interactions with NTP and TFIIS. *Mol Cell* 16(6):955–965.
7. Bricogne G, et al. (2012) *BUSTER Version 2.11.5* (Global Phasing, Cambridge).
8. Emsley P, Lohkamp B, Scott WG, Cowtan K (2010) Features and development of Coot. *Acta Crystallogr D Biol Crystallogr* 66(Pt 4):486–501.
9. Wu X, Rossettini A, Hanes SD (2003) The ESS1 prolyl isomerase and its suppressor BYE1 interact with RNA pol II to inhibit transcription elongation in Saccharomyces cerevisiae. *Genetics* 165(4):1687–1702.
10. Donovan S, Harwood J, Drury LS, Diffley JF (1997) Cdc6p-dependent loading of Mcm proteins onto pre-replicative chromatin in budding yeast. *Proc Natl Acad Sci USA* 94 (11):5611–5616.
11. Keogh MC, et al. (2006) A phosphatase complex that dephosphorylates gammaH2AX regulates DNA damage checkpoint recovery. *Nature* 439(7075):497–501.
12. Rothbart SB, Krajewski K, Strahl BD, Fuchs SM (2012) Peptide microarrays to interrogate the "histone code". *Methods Enzymol* 512:107–135.
13. Tong AH, et al. (2001) Systematic genetic analysis with ordered arrays of yeast deletion mutants. *Science* 294(5550):2364–2368.
14. Tong AH, et al. (2004) Global mapping of the yeast genetic interaction network. *Science* 303(5659):808–813.
15. Giaever G, et al. (2002) Functional profiling of the Saccharomyces cerevisiae genome. *Nature* 418(6896):387–391.
16. Seizl M, Larivière L, Pfaffeneder T, Wenzeck L, Cramer P (2011) Mediator head subcomplex Med11/22 contains a common helix bundle building block with a specific function in transcription initiation complex stabilization. *Nucleic Acids Res* 39(14): 6291–6304.
17. Ranish JA, Yudkovsky N, Hahn S (1999) Intermediates in formation and activity of the RNA polymerase II preinitiation complex: Holoenzyme recruitment and a postrecruitment role for the TATA box and TFIIB. *Genes Dev* 13(1):49–63.
18. Seizl M, et al. (2011) A conserved GA element in TATA-less RNA polymerase II promoters. *PLoS ONE* 6(11):e27595.
19. Damsma GE, Alt A, Brueckner F, Carell T, Cramer P (2007) Mechanism of transcriptional stalling at cisplatin-damaged DNA. *Nat Struct Mol Biol* 14(12):1127–1133.
20. Mayer A, et al. (2010) Uniform transitions of the general RNA polymerase II transcription complex. *Nat Struct Mol Biol* 17(10):1272–1278.
21. Fan X, Lamarre-Vincent N, Wang Q, Struhl K (2008) Extensive chromatin fragmentation improves enrichment of protein binding sites in chromatin immunoprecipitation experiments. *Nucleic Acids Res* 36(19):e125.
22. Aparicio O, et al. (2005) Chromatin immunoprecipitation for determining the association of proteins with specific genomic sequences in vivo. *Current Protocols in Molecular Biology,* ed Ausubel FM, et al. February; Chapter 21:Unit 21.3.

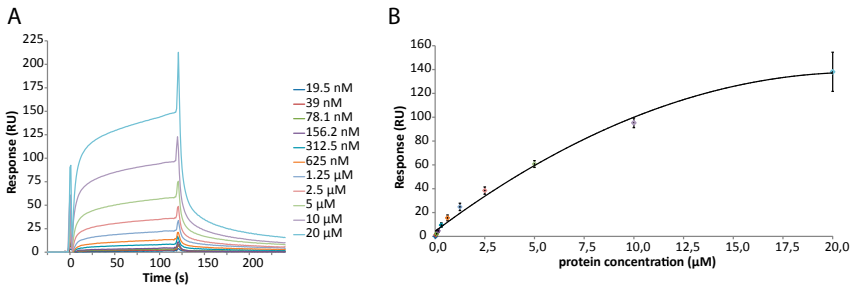

Fig. S1. Binding of full-length Bye1 to immobilized Pol II monitored by Surface Plasmon Resonance (SPR). (*A*) Time-resolved binding of Bye1 dilution series. For reasons of clarity, only one representative curve is shown for each measurement. All measurements have been carried out in triplicate. (*B*) Corresponding fitted curve (solid line). The curve is reference and blank subtracted. The unusual approach of immobilizing the larger component has been chosen due to limiting amounts of endogenously purified Pol II and to allow comparison of binding affinities of other transcription factors to Pol II (not discussed in this study).

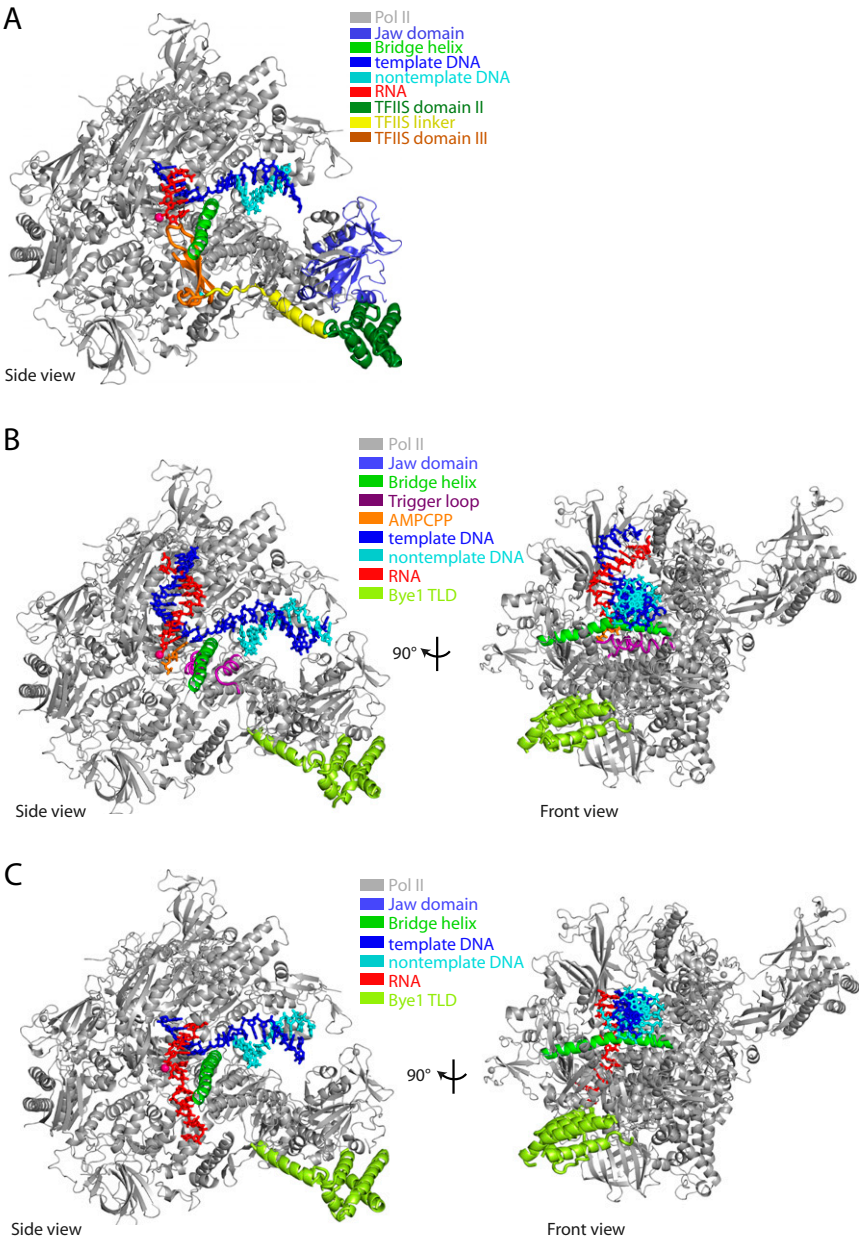

Fig. S2. Additional structures of Pol II complexes. (*A*) Structure of Pol II-TFIIS complex (5). (*B*) Ribbon model of the Pol II–Bye1 complex containing an additional nucleotide. (*C*) Ribbon model of the arrested Pol II–Bye1 complex.

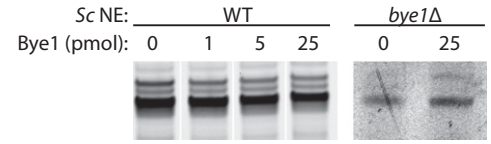

Fig. S3. Transcriptional activity of Bye1-depleted nuclear extracts. Transcriptional activities of WT and Bye1-depleted (*bye1*Δ) nuclear extracts (NE) in an in vitro transcription assay using a nucleosome-free DNA template. For experimental procedures, see *SI Materials and Methods*.

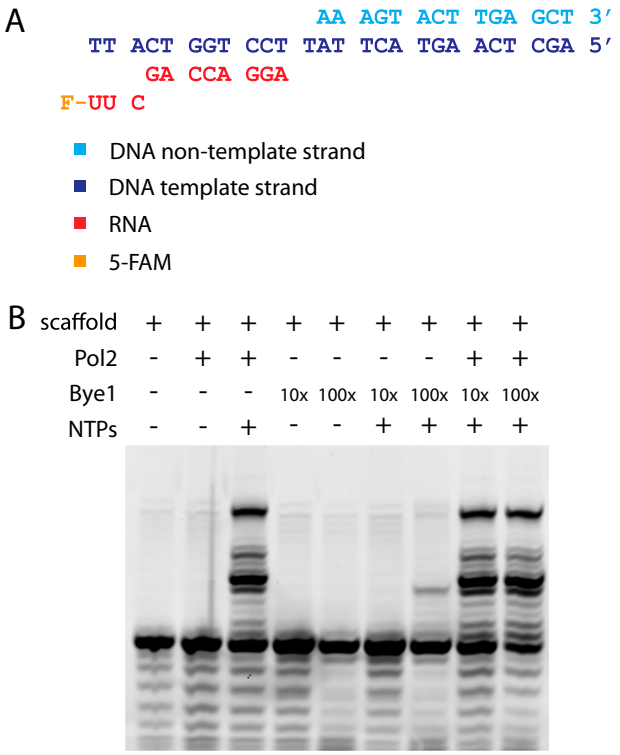

Fig. S4. Effect of Bye1 on Pol II elongation in vitro. (*A*) Nucleic acid scaffold for reconstitution of Pol II EC. (*B*) Gel electrophoresis separation of RNA products obtained in RNA extension assay. For experimental procedures, see *SI Materials and Methods*.

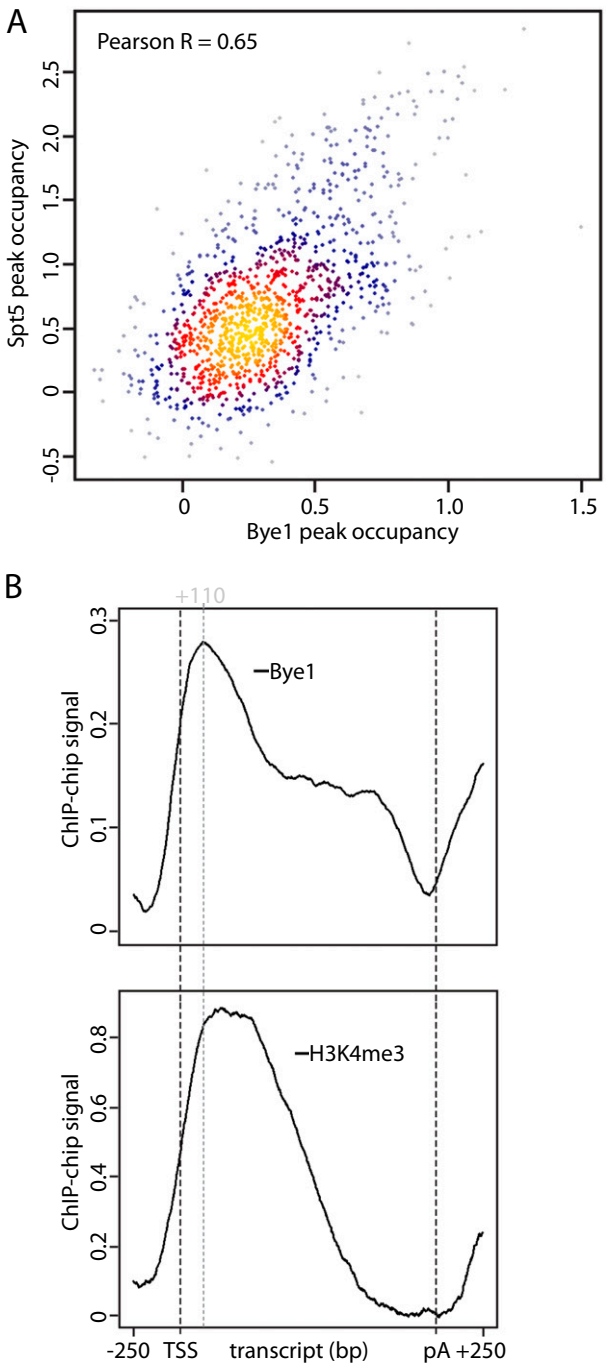

Fig. S5. ChIP-chip analysis of Bye1. (*A*) Correlation of Bye1 and Spt5 occupancies. (*B*) Comparison of Bye1 and H3K4me3 (1) occupancy profiles.

1. Schulze JM, et al. (2011) Splitting the task: Ubp8 and Ubp10 deubiquitinate different cellular pools of H2BK123. *Genes Dev* 25(21):2242–2247.

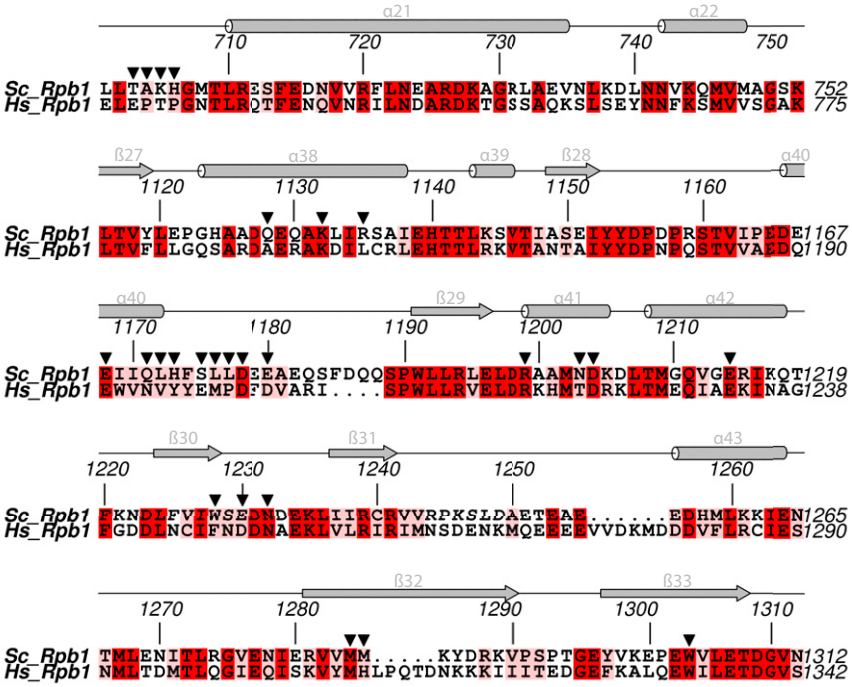

Fig. S6. Conservation of the Pol II–Bye1 interface in human homologs. Amino acid sequence alignments of *S. cerevisiae* Rpb1 and *Homo sapiens* Rpb1. Secondary structure elements are indicated as arrows (β-strands) or rods (α-helices). Loops are indicated with solid lines. Residues that are part of the Pol II–Bye1 interface are marked with black triangles.

Table S1. Diffraction data and refinement statistics

PDB ID	Pol II–Bye1 (4bxz)	Pol II EC–Bye1 TLD (4by7)	Pol II EC–Bye1 TLD + AMPCPP (4by1)	Arrested Pol II–Bye1 TLD (4bxx)
Data collection				
Space group	$C222_1$	$C222_1$	$C222_1$	$C222_1$
Unit cell axes (Å)	220.55	222.50	222.24	222.92
	392.09	390.68	391.58	392.67
	279.80	281.97	281.02	281.04
Unit cell angle (°)	$\alpha = \beta = \Upsilon = 90$	$\alpha = \beta = \Upsilon = 90$	$\alpha = \beta = \Upsilon = 90$	$\alpha = \beta = \Upsilon = 90$
Resolution range (Å)	49.63–4.80 (4.92–4.80)	48.84–3.15 (3.23–3.15)	48.95–3.60 (3.69–3.60)	49.08–3.28 (3.37–3.28)
Unique reflections	59,394 (4,352)	210,346 (15,471)	141,065 (10,391)	187,168 (13,766)
Completeness (%)	99.97 (100)	99.98 (100)	99.98 (100)	99.98 (99.98)
Redundancy	7.50 (7.82)	7.66 (7.74)	7.62 (7.61)	7.66 (7.49)
R_{sym} (%)	40.9 (173.0)	11.6 (165.2)	21.2 (193.4)	12.9 (185.4)
I/σ(I)	6.05 (1.24)	15.97 (1.60)	9.95 (1.57)	14.66 (1.52)
CC(1/2)	98.5 (60.8)	99.8 (63.2)	99.6 (56.3)	99.8 (67.1)
Refinement				
Non-H atoms	31,510	33,261	33,026	32,753
B-factor (mean)	199.00	115.07	125.08	120.50
Rmsd bonds	0.010	0.010	0.009	0.010
Rmsd angles	1.33	1.22	1.21	1.29
R_{cryst} (%)	19.06	18.94	17.49	17.98
R_{free} (%)	25.27	21.19	20.62	20.77

Values in parentheses are for the highest resolution shell. All data were collected with a radiation wavelength of 0.9188 Å.

Table S2. List of microarrayed peptides

Peptide no.	Residue range	Sequence	Annotation
P1	H3 1–20	AR^{2}TK^{4}QTAR^{8}K^{9}S^{10}TGGK^{14}APRK^{18}QL-K(Biot)-NH_2	H3 (1-20)
P2	H3 1–20	ARTKQTARKSTGGK(Ac)APRKQL-K(Biot)-NH_2	H3K14ac
P3	H3 1–20	ARTKQTARK(Ac)STGGKAPRKQL-K(Biot)-NH_2	H3K9ac
P4	H3 1–20	ARTK(Ac)QTARKSTGGKAPRKQL-K(Biot)-NH_2	H3K4ac
P5	H3 1–20	ARTK(Ac)QTARKSTGGK(Ac)APRKQL-K(Biot)-NH_2	H3K4ac + K14ac
P6	H3 1–20	ARTKQTARK(Ac)STGGK(Ac)APRKQL-K(Biot)-NH_2	H3K9ac + K14ac
P7	H3 1–20	ARTK(Ac)QTARK(Ac)STGGKAPRKQL-K(Biot)-NH_2	H3K4ac + K9ac
P8	H3 1–20	ARTK(Ac)QTARK(Ac)STGGK(Ac)APRKQL-K(Biot)-NH_2	H3K4ac + K9ac + K14ac
P10	H3 1–20	ARTKQTARKSTGGKAPRK(Ac)QL-K(Biot)-NH_2	H3K18ac
P11	H3 1–20	ARTKQTARKSTGGK(Ac)APRK(Ac)QL-K(Biot)-NH_2	H3K14ac + K18ac
P12	H3 1–20	ARTKQTARK(Ac)STGGKAPRK(Ac)QL-K(Biot)-NH_2	H3K9ac + K18ac
P13	H3 1–20	ARTK(Ac)QTARKSTGGKAPRK(Ac)QL-K(Biot)-NH_2	H3K4ac + K18ac
P14	H3 1–20	ARTKQTARK(Ac)STGGK(Ac)APRK(Ac)QL-K(Biot)-NH_2	H3K9ac + K14ac + K18ac
P15	H3 1–20	ARTK(Ac)QTARKSTGGK(Ac)APRK(Ac)QL-K(Biot)-NH_2	H3K4ac + K14ac + K18ac
P16	H3 1–20	ARTK(Ac)QTARK(Ac)STGGKAPRK(Ac)QL-K(Biot)-NH_2	H3K4ac + K9ac + K18ac
P17	H3 1–20	ARTK(Ac)QTARK(Ac)STGGK(Ac)APRK(Ac)QL-K(Biot)-NH_2	H3K4ac + K9ac + K14ac + K18ac
P18	H3 1–20	ARTK(Me_3)QTARKSTGGKAPRKQL-K(Biot)-NH_2	H3K4me3
P19	H3 1–20	ARTK(Me_3)QTARK(Ac)STGGKAPRKQL-K(Biot)-NH_2	H3K4me3 + K9ac
P20	H3 1–20	ARTK(Me_3)QTARKSTGGK(Ac)APRKQL-K(Biot)-NH_2	H3K4me3 + K14ac
P21	H3 1–20	ARTK(Me_3)QTARKSTGGKAPRK(Ac)QL-K(Biot)-NH_2	H3K4me3 + K18ac
P22	H3 1–20	ARTK(Me_3)QTARK(Ac)STGGK(Ac)APRKQL-K(Biot)-NH_2	H3K4me3 + K9ac + K14ac
P23	H3 1–20	ARTK(Me_3)QTARK(Ac)STGGKAPRK(Ac)QL-K(Biot)-NH_2	H3K4me3 + K9ac + K18ac
P24	H3 1–20	ARTK(Me_3)QTARKSTGGK(Ac)APRK(Ac)QL-K(Biot)-NH_2	H3K4me3 + K14ac + K18ac
P25	H3 1–20	ARTK(Me_3)QTARK(Ac)STGGK(Ac)APRK(Ac)QL-K(Biot)-NH_2	H3K4me3 + K9ac + K14ac + K18ac
P26	H3 1–20	ARpTK(Me_3)QTARK(Ac)STGGK(Ac)APRK(Ac)QL-K(Biot)-NH_2	H3T3p + K4me3 + K9ac + K14ac + K18ac
P27	H3 1–20	ARpTK(Me_3)QTARKSTGGKAPRKQL-K(Biot)-NH_2	H3T3p + K4me3
P28	H3 1–20	AR(Me_2a)pTK(Me_3)QTARK(Ac)STGGK(Ac)APRK(Ac)QL-K(Biot)-NH_2	H3R2me2a + T3p + K4me3 + K9ac + K14ac + K18ac
P29	H3 1–20	AR(Me_2a)pTK(Me_3)QTARKSTGGKAPRKQL-K(Biot)-NH_2	H3R2me2a + T3p + K4me3
P30	H3 1–20	AR(Me_2a)TK(Me_3)QTARKSTGGKAPRKQL-K(Biot)-NH_2	H3R2me2a + K4me3
P32	H3 1–20	ARTK(Me_2)QTARKSTGGKAPRKQL-K(Biot)-NH_2	H3K4me2
P33	H3 1–20	ARTK(Me_2)QTARK(Ac)STGGK(Ac)APRK(Ac)QL-K(Biot)-NH_2	H3K4me2 + K9ac + K14ac + K18ac
P34	H3 1–20	ARTK(Me)Q TARKSTGGKAPRKQL-K(Biot)-NH_2	H3K4me1
P35	H3 1–20	ARTK(Me)QTARK(Ac)STGGK(Ac)APRK(Ac)QL-K(Biot)-NH_2	H3K4me1 + K9ac + K14ac + K18ac
P36	H3 1–20	ARTKQTARKpSTGGKAPRKQL-K(Biot)-NH_2	H3S10p
P37	H3 1–20	ARTK(Ac)QTARK(Ac)pSTGGK(Ac)APRK(Ac)QL-K(Biot)-NH_2	H3K4ac + K9ac + S10p + K14ac + K18ac
P38	H3 1–20	ARTK(Me_3)QTARKpSTGGKAPRKQL-K(Biot)-NH_2	H3K4me3 + S10p
P39	H3 1–20	ARTK(Me_3)QTARK(Ac)pSTGGK(Ac)APRK(Ac)QL-K(Biot)-NH_2	H3K4me3 + K9ac + S10p + K14ac + K18ac
P40	H3 1–20	AR(Me_2a)TK(Me_3)QTARKpSTGGKAPRKQL-K(Biot)-NH_2	H3R2me2a + K4me3 + S10p
P41	H3 1–20	AR(Me_2a)TK(Me_3)QTARK(Ac)pSTGGK(Ac)APRK(Ac)QL-K(Biot)-NH_2	H3R2me2a + K4me3 + K9ac + S10p + K14ac + K18ac
P42	H3 1–20	ARTKQTARK(Me_3)STGGKAPRKQL-K(Biot)-NH_2	H3K9me3
P43	H3 1–20	ARTK(Ac)QTARK(Me_3)STGGK(Ac)APRK(Ac)QL-K(Biot)-NH_2	H3K4ac + K9me3 + K14ac + K18ac
P44	H3 1–20	ARTK(Me_2)QTARK(Ac)STGGKAPRK(Ac)QL-K(Biot)-NH_2	H3K4me2 + K9ac + K18ac
P45	H3 1–20	ARTK(Me)QTARK(Ac)STGGKAPRK(Ac)QL-K(Biot)-NH_2	H3K4me1 + K9ac + K18ac
P47	H3 1–20	AR(Me_2a)TKQTARKSTGGKAPRKQL-K(Biot)-NH_2	H3R2me2a
P48	H3 1–20	AR(Me_2a)TK(Ac)QTARK(Ac)STGGK(Ac)APRK(Ac)QL-K(Biot)-NH_2	H3R2me2a + K4ac + K9ac + K14ac + K18ac
P50	H3 1–20	AR(Me_2a)TK(Me_3)QTARK(Ac)STGGK(Ac)APRK(Ac)QL-K(Biot)-NH_2	H3R2me2a + K4me3 + K9ac + K14ac + K18ac
P51	H3 1–20	AR(Me)TK(Me_3)QTARKSTGGKAPRKQL-K(Biot)-NH_2	H3R2me1 + K4me3
P52	H3 1–20	AR(Me)TK(Me_3)QTARK(Ac)STGGK(Ac)APRK(Ac)QL-K(Biot)-NH_2	H3R2me1 + K4me3 + K9ac + K14ac + K18ac
P53	H3 1–20	ACitTKQTARKSTGGKAPRKQL-K(Biot)-NH_2	H3Cit2
P54	H3 1–20	ACitTK(Me_3)QTARKSTGGKAPRKQL-K(Biot)-NH_2	H3Cit2 + K4me3
P55	H3 1–20	ACitTK(Me_3)QTARK(Ac)STGGK(Ac)APRK(Ac)QL-K(Biot)-NH_2	H3Cit2 + K4me3 + K9ac + K14ac + K18ac
P56	H3 1–20	ACitTK(Ac)QTARK(Ac)STGGK(Ac)APRK(Ac)QL-K(Biot)-NH_2	H3Cit2 + K4ac + K9ac + K14ac + K18ac
P57	H3 1–20	ARpTKQTARKSTGGKAPRKQL-Peg-K(Biot)-NH_2	H3T3p
P58	H4 1–23	Ac-SGRGK^{5}GGKGLGKGGAKRHRKVLR-Peg-Biot	H4 (1-23)
P59	H4 1–23	Ac-SGRGK(Ac)GGK(Ac)GLGK(Ac)GGAK(Ac)RHRKVLR-Peg-Biot	H4K5ac + K8ac + K12ac + K16ac
P60	H3 1–20	AR(Me_2a)TK(Me_2)QTARKSTGGKAPRKQL-K(Biot)-NH_2	H3R2me2a + K4me2
P61	H3 1–20	AR(Me_2s)TK(Me_2)QTARKSTGGKAPRKQL-K(Biot)-NH_2	H3R2me2s + K4me2
P62	H3 1–20	AR(Me)TK(Me_2)QTARKSTGGKAPRKQL-K(Biot)-NH_2	H3R2me1 + K4me2
P63	H3 1–20	ACitTK(Me_2)QTARKSTGGKAPRKQL-K(Biot)-NH_2	H3Cit2 + K4me2
P66	H4 1–23	Ac-SGRGK(Ac)GGKGLGKGGAKRHRKVLR-Peg-Biot	H4K5ac
P67	H4 1–23	Ac-SGRGKGGK(Ac)GLGKGGAKRHRKVLR-Peg-Biot	H4K8ac

Table S2. Cont.

Peptide no.	Residue range	Sequence	Annotation
P68	H4 1–23	Ac-SGRGKGGKGLGK(Ac)GGAKRHRKVLR-Peg-Biot	H4K12ac
P69	H4 1–23	Ac-SGRGKGGKGLGKGGAK(Ac)RHRKVLR-Peg-Biot	H4K16ac
P70	H4 1–23	Ac-SGRGK(Ac)GGKGLGK(Ac)GGAKRHRKVLR-Peg-Biot	H4K5ac + K12ac
P71	H4 1–23	Ac-SGRGKGGK(Ac)GLGKGGAK(Ac)RHRKVLR-Peg-Biot	H4K8ac + K16ac
P72	H4 1–23	Ac-SGRGK(Ac)GGK(Ac)GLGK(Ac)GGAKRHRKVLR-Peg-Biot	H4K5ac + K8ac + K12ac
P73	H4 1–23	Ac-SGR(Me_2a)GKGGKGLGKGGAKRHRKVLR-K(Biot)-NH_2	H4R3me2a
P74	H4 1–23	Ac-SGR(Me_2s)GKGGKGLGKGGAKRHRKVLR-K(Biot)-NH_2	H4R3me2s
P75	H4 1–23	Ac-SGR(Me)GKGGKGLGKGGAKRHRKVLR-K(Biot)-NH_2	H4R3me1
P76	H4 1–23	Ac-pSGR(Me_2a)GKGGKGLGKGGAKRHRKVLR-K(Biot)-NH_2	H4S1p + R3me2a
P77	H4 1–23	Ac-pSGR(Me_2s)GKGGKGLGKGGAKRHRKVLR-K(Biot)-NH_2	H4S1p + R3me2s
P78	H4 1–23	Ac-pSGR(Me)GKGGKGLGKGGAKRHRKVLR-K(Biot)-NH_2	H4S1p + R3me1
P79	H4 1–23	Ac-SGR(Me_2a)GK(Ac)GGK(Ac)GLGK(Ac)GGAK(Ac)RHRK(Ac)VLR-K(Biot)-NH_2	H4R3me2a + K5ac + K8ac + K12ac + K16ac + K20ac
P80	H4 1–23	Ac-SGR(Me_2s)GK(Ac)GGK(Ac)GLGK(Ac)GGAK(Ac)RHRK(Ac)VLR-K(Biot)-NH_2	H4R3me2s + K5ac + K8ac + K12ac + K16ac + K20ac
P81	H4 1–23	Ac-SGR(Me)GK(Ac)GGK(Ac)GLGK(Ac)GGAK(Ac)RHRK(Ac)VLR-K(Biot)-NH_2	H4R3me1 + K5ac + K8ac + K12ac + K16ac + K20ac
P82	H4 11–27	Ac-GKGGAKRHRK(Me_3)VLRDNIQ-Peg-Biot	H4K20me3
P83	H4 11–27	Ac-GKGGAKRHRK(Me_2)VLRDNIQ-Peg-Biot	H4K20me2
P84	H4 11–27	Ac-GKGGAKRHRK(Me)VLRDNIQ-Peg-Biot	H4K20me1
P85	H4 11–27	Ac-GK(Ac)GGAK(Ac)RHRK(Me_3)VLRDNIQ-Peg-Biot	H4K12ac + K16ac + K20me3
P86	H4 11–27	Ac-GK(Ac)GGAK(Ac)RHRK(Me_2)VLRDNIQ-Peg-Biot	H4K12ac + K16ac + K20me2
P89	H3 1–20	ARTK(Me_3)QTAR(Me_2s)K(Me_3)STGGKAPRKQL-K(Biot)-NH_2	H3K4me3 + R8me2s + K9me3
P90	H3 15–43	Ac-APRK^{18}QLATK^{23}AARK^{27}SAPSTGGVK^{36}K^{37}PHRYGGK(Biot)-NH_2	H3 (15-41)
P91	H3 15–43	Ac-APRK(Me_3)QLATKAARKSAPSTGGVKKPHRY-GG-K(Biot)-NH_2	H3K18me3
P93	H3 15–43	Ac-APRKQLATKAARKSAPSTGGVK(Me_3)KPHRY-GG-K(Biot)-NH_2	H3K36me3
P95	H3 15–43	Ac-APRK(Me_3)QLATKAARKSAPSTGGVK(Me_3)KPHRY-GG-K(Biot)-NH_2	H3K18me3 + K36me3
P96	H3 1–20	ARTK(Me_3)QTAR(Me_2a)K(Me_3)STGGKAPRKQL-K(Biot)-NH_2	H3K4me3 + R8me2a + K9me3
P99	H4 11–27	Ac-GKGGAKRHRKVLRDNIQ-Peg-Biot	H4 (11-27)
P100	H3 74–84	Ac-IAQDFKTDLRF-Peg-K(Biot)-NH_2	H3 (74-84) *N*-ac
P101	H3 74–84	Ac-IAQDFK(Me_3)TDLRF-Peg-K(Biot)-NH_2	H3K79me3
P102	H3 74–84	Ac-IAQDFK(Me_2)TDLRF-Peg-K(Biot)-NH_2	H3K79me2
P103	H3 74–84	Ac-IAQDFK(Me)TDLRF-Peg-K(Biot)-NH_2	H3K79me1
P104	H3 74–84	IAQDFKTDLRF-Peg-K(Biot)-NH_2	H3 (74-84)
P120	H3 27–45	KSAPSTGGVK(Me_3)KPHRYKPGT-G-K(Biot)-NH_2	H3K36me3 (27-45)
P121	H3 27–45	KSAPSTGGVK(Me_2)KPHRYKPGT-GG-K(Biot)-NH_2	H3K36me2 (27-45)
P123	H3 27–45	KSAPSTGGVK(Ac)KPHRYKPGT-GG-K(Biot)-NH_2	H3K36ac (27-45)
P124	H3 27–45	KSAPSTGGVKKPHRYKPGT-GG-K(Biot)-NH_2	H3 (27-45)
P125	H3 1–20	ARpTKQTARKSTGGKAPRKQL-K(Biot)-NH_2	H3T3p
P129	H3 6–30	Ac-TARK(Me_2)STGGKAPRKQLATKAARK(Me_2)SAP-Peg-K(Biot)-NH_2	H3K9me2 + K27me2
P132	H3 1–20	ARTK(Me_3)QTARK(Me_3)STGGKAPRKQL-K(Biot)-NH_2	H3K4me3 + K9me3
P133	H3 1–20	ARTKQTARK(Me_2)STGGKAPRKQL-K(Biot)-NH_2	H3K9me2
P134	H3 1–20	ARTKQTARK(Me)STGGKAPRKQL-K(Biot)-NH_2	H3K9me1
P137	H3 1–20	ARTKQTARKSTGGKAPRK(Me_3)QL-K(Biot)-NH_2	H3K18me3
P138	H3 1–20	ARTKQTARKSTGGKAPRK(Me_2)QL-K(Biot)-NH_2	H3K18me2
P139	H3 1–20	ARTKQTARKSTGGKAPRK(Me)QL-K(Biot)-NH_2	H3K18me1
P144	H3 1–20	ARTKQTARK(Ac)pSTGGKAPRKQL-K(Biot)-NH_2	H3K9ac + S10p
P145	H3 1–20	ARTKQTARK(Me_3)pSTGGKAPRKQL-K(Biot)-NH_2	H3K9me3 + S10p
P146	H3 1–20	ARTKQTARK(Me_2)pSTGGKAPRKQL-K(Biot)-NH_2	H3K9me2 + S10p
P147	H3 1–20	ARTKQTARK(Me)pSTGGKAPRKQL-K(Biot)-NH_2	H3K9me1 + S10p
P148	H3 1–20	ARTK(Me_3)QTARK(Ac)pSTGGKAPRKQL-K(Biot)-NH_2	H3K4me3 + K9ac + S10p
P149	H3 1–22	ARTKQTARKSTGGKAPR(Me_2a)KQLAT-K(Biot)-NH_2	H3R17me2a
P150	H3 1–22	ARTKQTARKSTGGKAPR(Me_2s)KQLAT-K(Biot)-NH_2	H3R17me2s
P151	H3 1–22	ARTKQTARKSTGGKAPR(Me)KQLAT-K(Biot)-NH_2	H3R17me1
P157	H3 1–20	AR(Me_2s)TK(Me_3)QTARKSTGGKAPRKQL-K(Biot)-NH_2	H3R2me2s + K4me3
P162	H3 1–20	ARTKQpTARKSTGGKAPRKQL-K(Biot)-NH_2	H3T6p
P163	H3 1–20	ARTK(Me_3)QpTARKSTGGKAPRKQL-K(Biot)-NH_2	H3K4me3 + T6p
P164	H3 1–20	ARTK(Me_2)QpTARKSTGGKAPRKQL-K(Biot)-NH_2	H3K4me2 + T6p
P165	H3 1–20	ARTKQpTARK(Ac)STGGK(Ac)APRK(Ac)QL-K(Biot)-NH_2	H3T6p + K9ac + K14ac + K18ac
P166	H3 1–20	ARTK(Me_3)QpTARK(Ac)STGGK(Ac)APRK(Ac)QL-K(Biot)-NH_2	H3K4me3 + T6p + K9ac + K14ac + K18ac
P167	H3 1–20	ARTK(Me_2)QpTARK(Ac)STGGK(Ac)APRK(Ac)QL-K(Biot)-NH_2	H3K4me2 + T6p + K9ac + K14ac + K18ac

Table S2. Cont.

Peptide no.	Residue range	Sequence	Annotation
P174	H3 1–20	AR(Me_2s)TK(Me_3)QTARK(Ac)STGGK(Ac)APRK(Ac)QL-K(Biot)-NH_2	H3R2me2s + K4me3 + K9ac + K14ac + K18ac
P178	H3 1–20	ARTKQTAR(Me)K(Me_3)STGGKAPRKQL-K(Biot)-NH_2	H3R8me1 + K9me3
P179	H3 1–20	ARTKQTAR(Me)K(Me_2)STGGKAPRKQL-K(Biot)-NH_2	H3R8me1 + K9me2
P180	H3 1–20	ARTKQTAR(Me_2a)K(Me_3)STGGKAPRKQL-K(Biot)-NH_2	H3R8me2a + K9me3
P181	H3 1–20	ARTKQTAR(Me_2a)K(Me_2)STGGKAPRKQL-K(Biot)-NH_2	H3R8me2a + K9me2
P182	H3 1–20	ARTKQTAR(Me_2a)K(Me)STGGKAPRKQL-K(Biot)-NH_2	H3R8me2a + K9me1
P183	H3 1–20	ARTKQTAR(Me_2s)K(Me_3)STGGKAPRKQL-K(Biot)-NH_2	H3R8me2s + K9me3
P184	H3 1–20	ARTKQTAR(Me_2s)K(Me_2)STGGKAPRKQL-K(Biot)-NH_2	H3R8me2s + K9me2
P185	H3 1–20	ARTKQTAR(Me_2s)K(Me)STGGKAPRKQL-K(Biot)-NH_2	H3R8me2s + K9me1
P186	H3 1–20	ARTK(Ac)QTARK(Me_2)STGGK(Ac)APRK(Ac)QL-K(Biot)-NH_2	H3K4ac + K9me2 + K14ac + K18ac
P187	H3 1–20	ARTK(Ac)QTARK(Me)STGGK(Ac)APRK(Ac)QL-K(Biot)-NH_2	H3K4ac + K9me1 + K14ac + K18ac
P195	H3 15–34	Ac-APRK^{18}QLATK^{23}AARK(Me_3)^{27}SAPSTGG-Peg-Biot	H3K27me3
P196	H3 15–34	Ac-APRK^{18}QLATK^{23}AARK(Me_2)^{27}SAPSTGG-Peg-Biot	H3K27me2
P197	H3 15–34	Ac-APRK^{18}QLATK^{23}AARK(Me)^{27}SAPSTGG–Peg-Biot	H3K27me1
P198	H3 15–34	Ac-APRK^{18}QLATK^{23}AAR(Me_2a)K(Me_3)^{27}SAPSTGG–Peg-Biot	H3R26me2a + K27me3
P200	H3 15–34	Ac-APRK^{18}QLATK^{23}AARR(Me_2a)K(Me)^{27}SAPSTGG-Peg-Biot	H3R26me2a + K27me1
P220	H3 1–20	ARTKQpTARK(Me_3)STGGKAPRKQL-K(Biot)-NH_2	H3T6p + K9me3
P221	H3 1–20	ARTKQpTAR(Me_2a)K(Me_3)STGGKAPRKQL-K(Biot)-NH_2	H3T6p + R8me2a + K9me3
P224	H3 15–34	Ac-APRK^{18}QLATK^{23}AAR(Me_2a)K^{27}SAPSTGG-Peg-Biot	H3R26me2a
P225	H3 15–34	Ac-APRK^{18}QLATK^{23}AARK(Me_3)^{27}pSAPSTGG-Peg-Biot	H3K27me3 + S28p
P226	H3 15–34	Ac-APRK^{18}QLATK^{23}AARK(Me_2)^{27}pSAPSTGG-Peg-Biot	H3S27me2 + S28p
P229	H3 1–20	ARTK(Ac)QTARK(Me_3)STGGKAPRKQL-K(Biot)-NH_2	H3K4ac + K9me3
P237	H3 1–32	ARTKQTARK(Me_2)STGGKAPRKQLATKAARKSAPAT-Peg-Biot	H3K9me2 (1-32)
P241	H3 15–34	Ac-APRK^{18}QLATK^{23}AARK(Ac)^{27}SAPSTGG-Peg-Biot	H3K27ac
P242	H3 15–34	Ac-APRK^{18}QLATK^{23}AARK(Ac)^{27}pSAPSTGG-Peg-K(Biot)-NH_2	H3K27ac + S28p
P243	H3 15–34	Ac-APRK^{18}QLATK^{23}AARK^{27}pSAPSTGG-Peg-K(Biot)-NH_2	H3S28p
P253	H3 52–61	Ac-RRYQK^{56}STELL-Peg-Biot	H3 (52-61)
P254	H3 52–61	Ac-RRYQK(Ac)STELL-Peg-Biot	H3K56ac (52-61)
P255	H3 52–61	Ac-RRYQK(Me_3)STELL-Peg-Biot	H3K56me3 (52-61)
P259	H3 1–15	ARTK(Me_2)QTARK(Me_2)STGGKA-Peg-Biot	H3K4me2 + K9me2
P260	H3 1–15	ARTK(Me)QTARK(Me_2)STGGKA-Peg-Biot	H3K4me1 + K9me2
P264	H3 1–15	ARTK(Me_3)QTARK(Me_2)STGGKA-Peg-Biot	H3K4me3 + K9me2
P300	H2A 1–17	Ac-SGRGKQGGKARAKAKTR-Peg-Biot	H2A (1–17)
P301	H2A 1–17	Ac-SGRGK(Ac)QGGK(Ac)ARAK(Ac)AK(Ac)TR-Peg-Biot	H2AK5ac + K9ac + K13ac + K15ac
P302	H2A 1–17	Ac-SGRGK(Ac)QGGKARAKAKTR-Peg-Biot	H2AK5ac
P303	H2A 1–17	Ac-pSGRGK(Ac)QGGKARAKAKTR-Peg-Biot	H2AS1p + K5ac
P304	H2A 1–17	Ac-SGR(Me_2a)GK(Ac)QGGKARAKAKTR-Peg-Biot	H2AR3me2a + K5ac
P305	H2A 1–17	Ac-pSGR(Me_2a)GK(Ac)QGGKARAKAKTR-Peg-Biot	H2AS1p + R3me2a + K5ac
P306	H2A 1–17	Ac-SGCitGK(Ac)QGGKARAKAKTR-Peg-Biot	H2ACit3 + K5ac
P307	H2A 1–17	Ac-pSGCitGK(Ac)QGGKARAKAKTR-Peg-Biot	H2AS1p + Cit3 + K5ac
P308	H2A 1–17	Ac-pSGRGK(Ac)QGGK(Ac)ARAK(Ac)AK(Ac)TR-Peg-Biot	H2AS1p + K5ac + K9ac + K13ac + K15ac
P309	H2A 1–17	SGRGK(Ac)QGGK(Ac)ARAK(Ac)AK(Ac)TR-Peg-Biot	H2AK5ac + K9ac + K13ac + K15ac (no *N*-ac)
P310	H2A 1–17	pSGRGK(Ac)QGGK(Ac)ARAK(Ac)AK(Ac)TR-Peg-Biot	H2AS1p + K5ac + K9ac + K13ac + K15ac (no *N*-ac)
P311	H2A.X	Biot-Peg-G^{132}KKATQAS^{139}QEY^{142}-OH	H2AX (132-142)
P312	H2A.X	Biot-Peg-G^{132}KKATQApS^{139}QEY^{142}-OH	H2AX (S139p)
P350	H4 1–23	Ac-SGR(Me_2a)GK(Ac)GGKGLGKGGAKRHRKVLR-K(Biot)-NH_2	H4R3me2a + K5ac
P351	H4 1–23	SGRGKGGKGLGKGGAKRHRKVLR-Peg-Biot	H4 (1-23) (no *N*-ac)
P352	H4 1–23	Ac-SGRGKGGKGLGKGGAKRHRK(Ac)VLR$_D$-Peg-Biot	H4K20ac
P353	H4 1–23	Ac-pSGRGK(Ac)GGK(Ac)GLGK(Ac)GGAK(Ac)RHRKVLR-Peg-Biot	H4S1p + K5ac + K8ac + K12ac + K16ac
P359	H4 1–23	Ac-SGRGK(Ac)GGK(Ac)GLGKGGAKRHRKVLR-Peg-Biot	H4K5ac + K8ac
P360	H4 1–23	Ac-SGRGK(Ac)GGKGLGKGGAK(Ac)RHRKVLR-Peg-Biot	H4K5ac + K16ac
P362	H4 1–23	Ac-SGRGKGGK(Ac)GLGK(Ac)GGAKRHRKVLR-Peg-Biot	H4K8ac + K12ac
P363	H4 1–23	Ac-SGRGKGGK(Ac)GLGKGGAKRHRK(Ac)VLR-Peg-Biot	H4K12ac + K16ac
P366	H4 1–23	Ac-SGRGKGGKGLGKGGAK(Ac)RHRK(Ac)VLR-Peg-Biot	H4K16ac + K20ac
P370	H4 1–23	Ac-SGRGQGGQGLGK(Ac)GGAQRHRQVLR-Peg-Biot	H4K12ac + KQ5,8,16,20
P371	H4 1–23	Ac-SGRGK(Me)GGKGLGKGGAKRHRKVLR-Peg-Biot	H4K5me1
P372	H4 1–23	Ac-SGRGKGGK(Me)GLGKGGAKRHRKVLR-Peg-Biot	H4K8me1
P373	H4 1–23	Ac-SGRGKGGKGLGK(Me)GGAKRHRKVLR-Peg-Biot	H4K12me1
P374	H4 1–23	Ac-SGRGK(Ac)GGK(Me)GLGK(Ac)GGAKRHRKVLR-Peg-Biot	H4K5ac + K8me1 + K12ac
P375	H4 1–23	Ac-SGRGK(Me)GGK(Ac)GLGK(Me)GGAKRHRKVLR-Peg-Biot	H4K5me1 + K8ac + K12me1
P376	H4 1–23	Ac-SGRGK(Me)GGK(Me)GLGK(Me)GGAKRHRKVLR-Peg-Biot	H4K5me1 + K8me1 + K12me1

Table S2. Cont.

Peptide no.	Residue range	Sequence	Annotation
P381	H4 1–23	Ac-SGRGK(Me)GGK(Ac)GLGK(Ac)GGAK(Ac)RHRKVLR-Peg-Biot	H4K5me1 + K8ac + K12ac + K16ac
P382	H4 1–23	Ac-SGRGK(Ac)GGK(Me)GLGK(Ac)GGAK(Ac)RHRKVLR-Peg-Biot	H4K5ac + K8me1 + K12ac + K16ac
P383	H4 1–23	Ac-SGRGK(Ac)GGK(Ac)GLGK(Me)GGAK(Ac)RHRKVLR-Peg-Biot	H4K5ac + K8ac + K12me1 + K16ac
P400	H2B 1–24	PEPAKSAPAPKKGSKKAVTKAQKK-Peg-Biot	H2B (1-24)
P401	H2B 1–24	PEPAK(Me_3)SAPAPKKGSKKAVTKAQKK-Peg-Biot	H2BK5me3
P402	H2B 1–24	PEPAK(Me_2)SAPAPKKGSKKAVTKAQKK-Peg-Biot	H2BK5me2
P403	H2B 1–24	PEPAK(Me)SAPAPKKGSKKAVTKAQKK-Peg-Biot	H2BK5me1
P625	H2A.X	Ac-SGRGKTGGKARAKAKSR-Peg-Biotin	H2A.X (1–17)
P626	H2A.X	Ac-SGRGK(Ac)TGGKARAKAKSR-Peg-Biotin	H2A.X K5ac
P789	H3 27–46	KSAPSTGGVK(Me_3)KPHRYRPGTV-K(biotin)-NH_2	H3K36me3
P790	H3 27–46	KSAPpSTGGVK(Me_3)KPHRYRPGTV-K(biotin)-NH_2	H3S31p + K36me3
Tags	Flag-Tag	Biot-Peg-DYKDDDDK-NH_2	Flag-Tag
Tags	HA-Tag	Biot-Peg-YPYDVPDYASL-NH_2	HA-Tag
Tags	His-Tag	Biot-Peg-HHHHHH-NH_2	His-Tag
Tags	Myc-Tag	Biot-Peg-EQKLISEEDL-NH_2	Myc-Tag
Tags	V5-Tag	Biot-Peg-GKPIPNPLLGLDST-NH_2	V5-Tag